Paclitaxel and Cisplatin-Induced Neurotoxicity: A Protective Role of Acetyl-L-Carnitine

Claudio Pisano,[1] Graziella Pratesi,[2] Diletta Laccabue,[2] Franco Zunino,[2] Pietro Lo Giudice,[1] Augusta Bellucci,[1] Licia Pacifici,[1] Barbara Camerini,[1] Loredana Vesci,[1] Massimo Castorina,[1] Sandra Cicuzza,[1] Giovanni Tredici,[3] Paola Marmiroli,[3] Gabriella Nicolini,[3] Stefania Galbiati,[3] Menotti Calvani,[1] Paolo Carminati,[1] and Guido Cavaletti[3]

[1]Research and Development, Sigma-Tau S.p.A. Industrie Farmaceutiche Riunite, Rome; [2]Department of Experimental Oncology, Istituto Nazionale per lo Studio e la Cura dei Tumori, Milan; and [3]Department of Neuroscience and Biomedical Technologies, University of Milan "Bicocca," Monza, Italy

ABSTRACT

Purpose: **Antineoplastic drugs belonging to platinum or taxane families are severely neurotoxic, inducing the onset of disabling peripheral neuropathies with different clinical signs. Acetyl-L-carnitine (ALC) is a natural occurring compound with a neuroprotective activity in several experimental paradigms. In this study we have tested the hypothesis that ALC may have a protective role on cisplatin and paclitaxel-induced neuropathy.**

Experimental Design: **Sensory nerve conduction velocity (SNCV) was measured in rats before, at end, and after an additional follow-up period from treatments with cisplatin, paclitaxel, or with the respective combination with ALC. In addition, serum from treated animals was collected to measure the levels of circulating NGF, and left sciatic nerves were processed for light and electron microscope observations. ALC interference on cisplatin and paclitaxel antitumor activity and protective mechanisms were investigated using several *in vitro* and *in vivo* models.**

Results: **ALC cotreatment was able to significantly reduce the neurotoxicity of both cisplatin and paclitaxel in rat models, and this effect was correlated with a modulation of the plasma levels of NGF in the cisplatin-treated animals. Moreover, experiments in different tumor systems indicated the lack of interference of ALC in the antitumor effects of cisplatin and paclitaxel. The transcriptional profile of gene expression in PC12 cells indicated that ALC, in the presence of NGF, was able to positively modulate NGFI-A expression, a gene relevant in the rescue from tissue-specific toxicity. Finally, the transcriptionally ALC-mediated effects were correlated to increase histone acetylation.**

Conclusion: **In conclusion, our results indicate that ALC is a specific protective agent for chemotherapy-induced neuropathy after cisplatin or paclitaxel treatment without showing any interference with the antitumor activity of the drugs.**

INTRODUCTION

The pathogenesis of antineoplastic drug-induced peripheral neuropathies is still poorly understood, although recent reports have lead to the hypothesis of possible mechanisms of the toxic action of some of these drugs. Cisplatin, the first platinum-derived drug to be used in clinical practice, induces a severe and dose-limiting sensory neuropathy due to damage of the primary sensory neurons of the DRG[4] where it forms DNA adducts (1).

The hypothesis of a relationship between NTs and cisplatin neurotoxicity has been supported recently by the finding that the circulating levels of one of the NT family members, *i.e.*, NGF, is markedly reduced in neuropathic cancer patients, which have been treated with different neurotoxic combinations of platinum-based chemotherapy schedules (2). Moreover, Aloe *et al.* (3) demonstrated that constitutive levels of NGF are reduced in several non-neural peripheral tissues during chronic cisplatin treatment in mice. More recently, Cavaletti *et al.* (4) evidenced that NGF levels, but not the level of other NTs such as brain-derived neurotrophic factor, NT-3, and NT-4/5, are specifically modulated during the course of cisplatin administration and return to normal levels after recovery from the neurotoxic damage. Several attempts have been made to prevent or reduce the neurotoxicity of cisplatin, and among other substances, some NTs have also been evaluated (5), demonstrating a protective effect of NGF (3, 6–8), a substance that exerts a strong trophic effect on DRG neuron subpopulations during development and, in particular conditions, possibly also during adulthood (5).

Taxanes are another family of neurotoxic antineoplastic agents. Their major mechanism of antineoplastic action (*i.e.*, enhancement of tubulin polymeration) is likely to be also one of the mechanisms at the basis of neurotoxicity, although antitubulin action is probably not the only mechanism of the neurotoxicity of paclitaxel and docetaxel (9). Thus far, no correlation

Received 2/20/03; revised 7/25/03; accepted 7/29/03.
The costs of publication of this article were defrayed in part by the payment of page charges. This article must therefore be hereby marked *advertisement* in accordance with 18 U.S.C. Section 1734 solely to indicate this fact.

Requests for reprints: Dr. Claudio Pisano, Department of Oncology, Research and Development, Sigma-Tau S.p.A. Industrie Farmaceutiche Riunite, Via Pontina, km 30.400, Pomezia (Rome), Italy. Phone: 39-06-91-39-37-60; Fax: 39-02-06-91-39-39-88; E-mail: claudio.pisano@sigmatau.it.

[4] The abbreviations used are: DRG, dorsal root ganglia; ALC, acetyl-L-carnitine; SNCV, sensory nerve conduction velocity; NGF, nerve growth factor; NT, neurotrophin; CTRL, control; %ILS, percentage increase in life span; %TVI, percentage tumor volume inhibition; BW, body weight.

has been evidenced between taxane neurotoxicity and changes in NT levels in tissues or in plasma. However, a relationship is suggested by the results of Apfel *et al.* (10) who demonstrated a reduction in the severity of paclitaxel-induced neuropathy in NGF-treated mice.

ALC is a member of the family of carnitines, a group of natural compounds that have an essential role in intermediary metabolism (11–14). Results from different experimental paradigms suggest a putative neuroprotective role for ALC. In fact, exogenous administration of ALC produces a positive effect on diabetic neuropathy (15–17), on motoneuron survival after axotomy (18), on the control of NGF level in the central nervous system of adult rats after total fimbria-fornix transection (19), and in the rate of transcription of the gene coding for the $p75^{NGFR}$ in the basal forebrain and cerebellum of aged rats (20). However, the pleiotropicity of effects associated with ALC cannot be explained solely on the basis of the above mentioned effects on intermediary metabolism. Over the last few years, the possibility has emerged that ALC may also be involved in nuclear events. Moreover, the molecular properties of ALC have led to the suggestion that it may play a role in histone acetylation and consequently in facilitating gene expression (21, 22).

In this study, we tested *in vivo* in two animal models of cisplatin- and paclitaxel-induced neuropathy the hypothesis that ALC may have a protective role on chemotherapy-induced neuropathy, and we examined whether ALC determines a modulation of NGF circulating levels in these models. Moreover, we examined the effect of ALC on the antitumor activity of cisplatin and paclitaxel using different *in vivo* models. Finally, we explored *in vitro* some putative mechanisms, which might be involved in the neuroprotective effect of ALC using rat neuronal-like cell lines.

MATERIALS AND METHODS

Drugs. Cisplatin (Platinex®) and paclitaxel (Taxol®) were purchased from Bristol-Myers-Squibb. ALC was supplied by Sigma-Tau (Pomezia, Italy).

In all of the *in vivo* experiments ALC was administered at a dose of 100 mg/kg p.o. dissolved in buffered saline solution in a volume of 10 ml/kg. Control animals were treated with 10 ml/kg of buffered saline solution.

Animal Husbandry. Animals were housed in a limited access animal facility. Animal room temperature and relative humidity were set at 22 ± 2°C and 55 ± 10% respectively. Artificial lighting provided a 24-h cycle of 12 h light/12 h dark (7 a.m. to 7 p.m.). The care and husbandry of animals were in accordance with European Directives no. 86/609, and with Italian D.L. 116, January 27th, 1992. All of the experiments were approved by the Ethics Committee for Animal Experimentation of the Istituto Nazionale Tumori or by the Sigma-Tau veterinarian.

In Vivo Neurotoxicity Studies in Rats

Paclitaxel Model. Twenty-four female Wistar rats (200–220 g at the beginning of the experiment; Charles River Lab, Calco, Italy) were divided by random selection into three groups: paclitaxel, paclitaxel + ALC, and CTRL groups. Paclitaxel was dissolved in cremophor/ethanol (50%/50%), and paclitaxel group rats ($n = 8$) were treated with 5 mg/kg i.v. on days 1, 2, 3, 9, and 10 using a volume of 0.8 ml/kg via a catheter implanted into the jugular vein (23). Animals of the paclitaxel + ALC group ($n = 8$) were treated with the same schedule of paclitaxel, but ALC was administered daily p.o. by gavage, starting 5 days before the first paclitaxel administration and until the end of the treatment period. Controls ($n = 8$) received only sham i.v. injections of the paclitaxel solvent.

Before starting the treatment and after the end of the treatment period (*i.e.*, on day 12) each animal underwent the determination of SNCV in the tail as described previously (24–26), using a method that was already used in previous experiments on neuroprotection (25, 26). Briefly, the antidromic SNCV in the tail nerve was assessed by placing recording ring electrodes distally in the tail, whereas the stimulating ring electrodes were placed 5 cm and 10 cm proximally with respect to the recording point. The latencies of the potentials recorded at the two sites after nerve stimulation were determined (peak-to-peak), and SNCV was calculated accordingly. All of the neurophysiological determinations were performed under standard conditions in a temperature-controlled room.

At the end of the experiment the animals from each group were sacrificed under general xylazine/ketamine anesthesia. The left sciatic nerves of rats from each group were obtained from the sacrificed animals and processed according to protocols reported previously (23), resin embedded, and used for light and electron microscope observations.

Cisplatin Model. Forty-five female Wistar rats (200–220 g at the beginning of the experiment; Charles River Lab) were divided by random selection into three groups: cisplatin, cisplatin + ALC, and CTRL groups. Cisplatin was dissolved in sterile saline, and cisplatin group rats ($n = 15$) were treated with cisplatin 2 mg/kg i.p. twice a week for eight times using a volume of 4 ml/kg (24–26). Animals of the cisplatin + ALC group ($n = 15$) were treated with the same dose of cisplatin, but ALC was administered daily p.o. by gavage, starting 5 days before the first cisplatin administration and until the end of the treatment period. Controls ($n = 15$) received only sham i.p. injections of the solvent. Before starting the treatment, at the end of the treatment (*i.e.*, at week 5), and after an additional follow-up period of 5 weeks, each animal underwent the determination of SNCV in the tail as described previously.

At week 5, 6 animals from each group were sacrificed under general xylazine/ketamine anesthesia, whereas all of the remaining animals in each group were sacrificed after the follow-up examination.

The left L5 DRG of rats sacrificed immediately after treatment were obtained and processed according to protocols reported previously (24–26), resin embedded, and used for light and electron microscope observations and for morphometry. On 1-μm thick semithin sections morphometric determinations of the cross-sectional area of the somata, nuclei, and nucleoli of 300 DRG neurons in each group were performed using an automatic image analyzer (Tas Plus, Leica GmbH, Solms, Germany; Refs. 24–26). Determinations were performed by a blinded examiner as to the treatment group using the same methods used in a previous experiment on neuroprotection (25, 26). At the sacrifice, 3 ml of whole blood were obtained from each animal through abdominal aorta puncture and collected into a heparinated tube. Plasma was obtained and immediately

stored at −80° until it was used for NGF level determination. The circulating levels of NGF were measured by ELISA using commercially available kits (E_{max} ImmunoAssay System; Promega, Madison WI; plasma working dilution for NGF 1:80) following the manufacturer's protocols.

Statistical Analysis. In the neurotoxicological studies the differences between all of the experimental groups in BW, SNCV, NGF circulating levels, and those observed in the morphometric data obtained in DRG were statistically evaluated using the ANOVA and the Tukey-Kramer post-test (significance level set at $P < 0.05$).

Antitumor Activity Studies of Cisplatin and Taxol in Combination with ALC

Cell Culture and Cytotoxicity Assay. Human tumor cell lines were used in the study. The NCI-H460 non-small cell lung carcinoma, HT-29 colon adenocarcinoma, PC3 prostate carcinoma, A2780 ovarian carcinoma, and HeLa cervix uteri carcinoma were grown in RPMI 1640 (Sigma Chemicals Aldrich, Milan, Italy). Human ovarian carcinoma IGROV-1 cells and human breast adenocarcinoma MDA-MB435 cells were grown in DMEM (Life Technologies, Inc.-Invitrogen, Paisley, United Kingdom). The NTERA-2 testicular teratocarcinoma cells were grown in Vitacell DMEM (American Type Culture Collection, Manassas, VA). All of the media contained 10% fetal bovine serum and 50 μg/ml gentamicin sulfate.

For the cytoxicity assay, cells were seeded in 96-well tissue culture plates (Corning, New York, NY) and were allowed to attach and recover for at least 24 h. Varying concentrations of drugs alone or combined with ALC (200 μg/ml) corresponding to 1 mM were then added to each well. The plates were incubated for 2 h and then washed before being incubated without drugs for an additional 72 h. The number of surviving cells was then determined by staining with sulfurhodamine B (27). $IC_{50} \pm$ SD were evaluated using an "ALLFIT" computer program.

***In Vivo* Experiments.** Murine Lewis lung carcinoma (3LL) was injected i.m. (1×10^5 cells/100 μl/mouse) into the right hind leg muscle of C57BL/6J mice (Charles River Lab) either for line maintenance or for antitumor activity experiments. Cisplatin was administered at the doses of 8 and 6 mg/kg 1 and 3 days after tumor implant. ALC 100 mg/kg was given daily by oral gavage for 14 days starting on the same day as the tumor implant.

Human tumor xenografts were also used in the study, *i.e.*, the NCI-H460 human lung carcinoma, the LoVo colon carcinoma, and the IGROV-1 and A2780 ovarian carcinomas. Tumors were maintained by s.c. passages of tumor fragments in flanks of nude athymic CD1 mice (Charles River Lab) as described previously (28). For chemotherapy experiments, tumor fragments were injected s.c. into both flanks of nude female CD1 mice. Each group included 4–5 mice bearing bilateral tumors. Cisplatin and paclitaxel were delivered by i.v. route according to their optimal schedules (*i.e.*, every 7^{th} day for 3 times for cisplatin and every 4^{th} day for 4 times for paclitaxel). ALC 100 mg/kg was delivered daily p.o. for 14–18 times, starting 3 days before the first treatment and ending 3 days after the last treatment with the cytotoxic drug.

The antitumor activity of the drugs alone or in combination with ALC was evaluated in terms of %ILS and %TVI in comparison with untreated controls. %ILS was calculated as follows: [(MST-treated group/MST control group) ×100] − 100, where MST is the median survival time. TVI was calculated as: %TVI = 100 − mean tumor volume of treated group/mean tumor volume of control group × 100, by measuring biweekly tumor diameters with a Vernier caliper. Tumor volume was calculated as: tumor volume (mm^3) = length (mm) × width $(mm)^2/2$, where the width and the length were the shortest and the longest diameters of each tumor, respectively. The animals were sacrificed by cervical dislocation when the mean tumor volume of the group was ~2 cm^3.

The general toxicity of the treatment was determined as BW loss percentage, calculated as: %BWL = 100 − (mean $BW_{day\ x}$/mean $BW_{day\ 1} \times 100$), where BW_x is the BW at the day of maximal loss during the treatment and BW_1 is the BW on the 1st day of treatment.

In the 3LL carcinoma model, the number of spontaneous lung metastases was also assessed. To perform this determination mice were sacrificed, and lungs were excised and fixed in Bouin's solution for 5 days. Tumor colonies on the surface of each of the 5 lobes were counted under a Zeiss dissection microscope.

Statistical Analysis. The experimental results were compared using the Mann-Whitney test or Student's *t* test. Differences were considered significant at $P < 0.05$.

Paclitaxel, Cisplatin, and ALC Treatment on Rat Pheochromocytoma PC12 Cell. Rat pheochromocytoma PC12 cells were obtained from the American Type Culture Collection. Cells were cultured in RPMI 1640 (Sigma Chemicals Aldrich, Milan, Italy) supplemented with 5% heat-inactivated horse serum (Life Technologies, Inc.-Invitrogen), 5% heat-inactivated FCS, and 1% penicillin streptomycin antibiotic mixture (Life Technologies, Inc.-Invitrogen) in a humidified incubator (Heraeus, Hanau, Germany) at 37°C with 5% CO_2 atmosphere. PC12 cells were seeded in six-well plates (containing a polilysinated coverslide) at a density of 150,000 cells/well. After 6 h cells were treated with NGF 100 ng/ml for 72 h to induce neuronal differentiation and neurite outgrowth. At the end of the period of incubation the medium was replaced and the differentiated cells were treated for 24 h with 100 ng/ml NGF ± paclitaxel (1 μg/ml) or cisplatin (10 μg/ml) ± ALC (1 mM; Ref. 29). PC12 cells were then fixed using the methanol-acetone method: cells grown on the cover slides were washed twice with PBS 1×, then treated with chilled methanol (−20°C) and incubated at +4°C for 2 min. Then the methanol was flushed out, and chilled acetone (−20°C) was put onto the cells. After 5 min, acetone was washed out and the cells were treated with 2 ml of 1% Triton X-100, 0.5% acetic acid in PBS 1× for 10 min at room temperature. Cells were washed twice with PBS 1× and incubated for 5 h with specific antiacetylated α-tubulin antibody (Sigma Immunochemicals) diluted 1:10 in PBS at room temperature in a humid chamber. After two rinses in PBS, cells were incubated overnight with FITC-labeled goat antimouse IgG antibody (Vector, Burlingame, CA) diluted 1:10 in PBS at room temperature to localize the neurites of differentiated cells and with Hoechst 1× for 10 min at room temperature to stain nuclei. The number of neurites of differentiated cells, *i.e.*, those >0.35 μm, was determined by a blinded examiner as to the treatment performed. Slides were analyzed with a Zeiss III

photomicroscope with epifluorescence equipment using the 09 combination of filters (BP 450–490, FT 510, LP420, or BP 546). Analysis was performed on 25 fields/treatment.

Atlas cDNA Expression Arrays and Northern Blot. For isolation of RNA, PC12 cells were plated at a density of 4×10^6 cells/flask (75 cm^2) 2 days before the treatment. Cells were then left untreated or treated for 2 h with 1 mM ALC or 1 ng/ml NGF or both. After treatments, total RNA was extracted from the PC12 cells using a TRIzol-based method (Life Technologies, Inc., Rockville, MD) according to the manufacturer's instructions.

RNA was treated with DNase according to the manufacturer's instructions (Ambion Inc., Austin, TX), and its quality was evaluated by denaturing formaldehyde/agarose gel electrophoresis, as well as by absorbance 260:280 ratios.

Polyadenylated RNA enrichment, probe synthesis, hybridization, and washing of the cDNA Atlas array membranes (Clontech, Palo Alto, CA) were carried out according to the instructions accompanying the macroarrays.

Arrays consisted of 1176 rat cDNA fragments (1.2 Atlas array), organized into broad functional groups. A complete list of the genes included on the membranes is available on the Clontech website.[5]

Briefly, 5 pg of RNA was used as template for cDNA synthesis, which was done in the presence of ^{32}P-labeled dATP (Amersham, Little Chalfont, England). The labeled probes were purified by spin column centrifugation (NucleoSpin Extraction Spin Column; Clontech), and hybridization was carried out at 68°C in a rotation hybridization oven. The membranes were then washed at 68°C and exposed for 1–3 days, and analyzed by a phosphoimaging system (STORM; Amersham).

Genes of which the expression changed 2-fold or more after treatment were included in our analysis. In Northern blot analysis total RNA (15–20 pg) was fractionated on 1.2% agarose gel, transferred onto nylon membrane (Boehringer Mannheim – Roche Diagnostic, Basel, Germany), and UV cross-linked to the filter (Stratalinker; Stratagene, La Jolla, CA). Northern blot filters were prehybridized in 0.5 mM Na_2HPO_4 (pH 7.2) with H_3PO_4, 1 mM EDTA, and 7% SDS at 65°C for 4 h. Hybridizations were carried out in the same buffer at 65°C for 18 h with the indicated cDNA probes. Sources of probes were the 4.8 Kb *Xho*I/*Bam*HI c-myc fragment (30), the 1.0 Kb *Eco*RI mouse glyceraldehyde-3-phosphate dehydrogenase fragment (31) and the 0.8 Kb NGFI-A fragment cloned in the *Pst*I site of the vector pUC9 (32). Each c-DNA (30 ng) was labeled with a [^{32}P]dCTP by random priming (Random Priming Kit; Boehringer Mannheim - Roche Diagnostic) and exposed in Phosphor Storage Screen by Molecular Dynamics. The autoradiograms were analyzed using the v. 3.3 PhosphorImager's ImageQuant software (Molecular Dynamics, Amersham).

Immunostaining of Acetylated Histones. PC12 cells were seeded in six-well plates (containing a polilysinated coverslide) at a density of 150,000 cells/well. Cells were untreated (control) or treated for 1 h with 1 mM ALC, 1 ng/ml NGF, 1 mM ALC plus 1 ng/ml NGF, or 100 ng/ml NGF. After the treatments, coverslides were rinsed twice in PBS (Dulbecco modified formula), fixed in ice-cold methanol for 5 min at 4°C, followed by 1 min in ice-cold acetone and permeabilized with 0.5% acetic acid, 1% Triton X-100 in PBS (pH 7.4) for 10 min at room temperature. After three washes of 5 min each in PBS, cells were immunostained by incubation for 1 h with the rabbit polyclonal IgG antihistone H4 antibody (Upstate, Lake Placid, NY) diluted 1 μg/ml in PBS at room temperature in a humid chamber. After two rinses in PBS, cells were incubated overnight with FITC-conjugated sheep antimouse IgG antibody (Amersham) diluted 1:10 in PBS at room temperature. Double immunostaining was performed using a rabbit polyclonal antihistone H4 antibody, specific for the acetylated isoform of H4 (Upstate; Ref. 33), diluted to 1 μg/ml in PBS and incubated for 3 h in a humid chamber at room temperature. The slides were then washed three times in PBS, incubated for 45 min with the secondary antibody (Texas red-labeled goat antirabbit IgG; Amersham) diluted to 1:50 in PBS, washed thoroughly with PBS, and mounted in 50% glycerol in PBS. Slides were analyzed with a Zeiss III photomicroscope with epifluorescence equipment, using the 09 combination of filters (BP 450–490, FT 510, LP420, or BP 546). Photographic images of two-color immunofluorescence were taken with a cooled CCD camera (Photometrics; Roper Scientific, PN Vianen, Netherlands) and processed using the IP-LAB Spectrum H-SU2 program on an Apple Power Macintosh 7100/80AV computer.

Cell Treatment with Labeled Compounds, Histone Purification, and SDS-PAGE. [^{14}C]ALC (50–60 mCi/mmol) and [^{14}C]sodium acetate (56.8 mCi/mmol) were purchased from New England Nuclear (Perkin-Elmer - Life Sciences Inc., Boston, MA).

Five $\times 10^6$ PC12 cells were pulse-labeled with 10 μCi of [^{14}C]ALC or [^{14}C]sodium acetate for 30 min in complete medium, then washed twice with fresh medium and cultured until harvesting in the same unlabeled medium. After 1 h, PC12 cells were lysed in buffer containing 10 mM Tris/HCl, 15 mM NaCl, 1 mM EDTA, 1% NP40, and 5 mM butyrate (pH 8.0). Nuclei were isolated according to Arends *et al.* (34). During the purification procedure, nuclei were examined by phase contrast microscopy to ascertain their purity grade. The native mixture of histones H1, H2A, H2B, H3, and H4 was isolated according to van der Westuyzen *et al.* (35). Electrophoresis in the presence of SDS was performed according to the procedure of Laemmli (36) on 10% polyacrylamide slab gels. Protein concentration was estimated according to the method of Bradford (37) using BSA as standard.

RESULTS

***In Vivo* Effect of ALC Treatment in Experimental Models of Peripheral Neuropathy Induced in the Rat by Administration of Cisplatin and Paclitaxel.** The putative neuroprotective effect of ALC was assessed in two well-characterized models of antineoplastic drug-induced peripheral neurotoxicity (23–26).

Paclitaxel Model. All of the animals completed the study. Animals in the CTRL group gained weight during the treatment period, whereas rats of the paclitaxel and paclitaxel + ALC groups maintained or even lost weight during the period of treatment (mean 208.6 g ± SD 12.0 and 208.7 ± 15.1, respec-

[5] Internet address: http://www.clontech.com.

Table 1 Effect of chemotherapy on neurologic parameters in young rats

Group[a]	SNCV[b] (mean ± SD) Day	SNCV[b] (mean ± SD) m/sec	NGF[c] (ng/ml)
Controls	35	41.1 ± 3.0	69.4 ± 12.7
Cisplatin	35	27.8 ± 1.9	42.7 ± 7.1[d]
Cisplatin + ALC	35	33.4 ± 2.8[e]	58.1 ± 15.3
Controls	12	33.0 ± 1.4	
Paclitaxel	12	27.5 ± 0.6	
Paclitaxel + ALC	12	31.2 ± 1.1[f]	

[a] Cisplatin: 2 mg/kg i.p., twice a week for 4 weeks from day 1; ALC: 100 mg/kg p.o., daily, starting 5 days before and ending the day of the last drug treatment; paclitaxel: 5 mg/kg i.v., on days 1, 2, 3, 9, and 10. Controls were treated with the drug solvent.
[b] SNCV in the tail nerve.
[c] Nerve Growth Factor level in rat plasma. Mean ± SD are reported.
[d] $P < 0.05$ *versus* controls.
[e] $P < 0.01$ *versus* controls.
[f] $P < 0.001$ compared with the corresponding drug-treated group.

Table 2 Morphometric evaluation of the dorsal root ganglia soma, nucleus, and nucleolus area in the cisplatin model (mean ± SD)

	Controls	Cisplatin	Cisplatin + ALC
Soma[a]	906.4 (407.4)	754.6[b] (398.4)	834.6[c] (457.0)
Nucleus[a]	136.2 (53.8)	116.9[b] (50.2)	126.8[c] (52.5)
Nucleolus[a]	11.7 (5.7)	8.1[b] (4.2)	10.1[b,d] (5.7)

[a] Expressed in μm^2.
[b] $P < 0.001$ *versus* controls.
[c] $P =$ not significant *versus* controls.
[d] $P < 0.001$ *versus* cisplatin.

tively; controls 229.8 ± 11.4, $P < 0.05$ *versus* both treated groups). In CTRL rats there was a mild increase in SNCV during the 12-day observation period (Table 1). After treatment SNCV was reduced significantly in comparison with the CTRL group in both paclitaxel and paclitaxel + ALC groups. The difference, however, was less marked in the paclitaxel + ALC group (mean CTRL group 33.0 m/sec ± SD 1.4, paclitaxel group 27.5 ± 0.6, $P < 0.001$ *versus* CTRL, paclitaxel + ALC group 31.2 ± 1.1, $P < 0.05$ *versus* CTRL). The difference between the two groups of paclitaxel-treated rats was highly significant in favor of ALC cotreatment ($P < 0.001$). The examination of the sciatic nerves at the light microscope confirmed previous observations (26), and evidenced in both the paclitaxel and paclitaxel + ALC groups very mild axonal degeneration, associated with "reactive" changes in Schwann cells, which had an enlarged cytoplasm. At the ultrastructural level, intra-axonal accumulation of aggregated microtubules were observed in some fibers in both paclitaxel-treated groups.

Cisplatin Model. All of the animals completed the study. Animals in the CTRL group gained weight at a steady rate during the entire observation time, whereas there was a marked weight reduction in both the cisplatin + ALC group and in cisplatin-treated rats (mean weight 183.9 g ± SD 27.0 and 186.3 ± 27.0, respectively; controls 246.0 ± 14.4, $P < 0.001$ *versus* both treated groups). At the end of the follow-up period no significant differences were seen among the three groups. In CTRL rats there was an increase in SNCV during the observation period (Table 1). The observed increase is a well-known feature in this model and is due to the maturation of the peripheral nervous system of these young adult rats. At the end of the treatment period, SNCV was significantly reduced in comparison with the CTRL group in both cisplatin and cisplatin + ALC groups ($P < 0.001$ for both groups). The difference, however, was significantly less marked in the cisplatin + ALC group (mean CTRL group 41.1 m/sec ± SD 3.0, cisplatin group 27.8 ± 1.9, and cisplatin + ALC group 33.4 ± 2.8), and the difference between the two groups of cisplatin-treated rats was significantly in favor of the ALC cotreatment ($P < 0.01$).

The features of CDDP-induced neuronopathy have already been reported in detail (24–26). In this experiment it was confirmed that the main pathological changes involved the DRG neurons, where the nucleolus and the nucleus underwent evident changes (*i.e.*, nucleolar segregation and an increased incidence of multinucleolated cells). On the contrary, the neuronal cytoplasmic involvement was very limited. The satellite cells were even less severely involved although, also in this case, the most prominent changes were evident in the nucleus, where a thinning of the chromatin layer was frequently observed. All of the

Table 3 Cytotoxicity of paclitaxel and cisplatin alone and in combination with ALC on different human tumor cell lines (IC_{50} as μg/ml ± SD)

Cells were treated for 2 h with paclitaxel or cisplatin at different concentrations ± 200 μg/ml ALC. Then the drugs were removed and fresh medium added. After 72 h cytotoxicity was evaluated with the sulphorodamine B test.

Tumor cell line	ALC	Drugs	ALC + drugs
Breast cancer (MDA-MB435)			
Paclitaxel	>200	0.005 ± 0.0002	0.005 ± 0.0002
Cisplatin	>200	6.2 ± 1.0	6.2 ± 0.09
Colon cancer (HT-29)			
Paclitaxel	>200	0.01 ± 0.001	0.01 ± 0.001
Cisplatin	>200	5.5 ± 0.04	4.3 ± 0.02
Prostate cancer (PC3)			
Paclitaxel	>200	0.03 ± 0.006	0.03 ± 0.006
Cisplatin	>200	7.1 ± 0.03	5.8 ± 0.1
Ovarian cancer (A2780)			
Paclitaxel	>200	0.08 ± 0.01	0.1 ± 0.01
Cisplatin	>200	0.2 ± 0.08	0.3 ± 0.01
Ovarian cancer (IGROV-1)			
Paclitaxel	>200	0.3 ± 0.06	0.3 ± 0.05
Cisplatin	>200	1.2 ± 0.08	1.8 ± 0.05
Cervix uteri cancer (HeLa)			
Paclitaxel	>200	0.1 ± 0.008	0.08 ± 0.007
Cisplatin	>200	1.6 ± 0.03	1.4 ± 0.07
NSCLC (NCI-H460)			
Paclitaxel	>200	0.1 ± 0.02	0.09 ± 0.03
Cisplatin	>200	1.3 ± 0.09	1.4 ± 0.1
Testicular teratocarcinoma (NTERA-2)			
Paclitaxel	>200	3.7 ± 0.3	3.2 ± 0.2
Cisplatin	>200	0.3 ± 0.03	0.3 ± 0.03

cited morphological changes occurred in the present experiment in both the cisplatin and cisplatin + ALC groups.

The morphometric determination of the somatic, nuclear, and nucleolar size performed on DRG neurons confirmed our previous observations in cisplatin-treated rats (24–26). In fact, after cisplatin treatment there was a significant reduction in all three of these parameters in the cisplatin group with respect to the CTRL group. The values in the cisplatin + ALC group always lay between those of the CTRL and the cisplatin groups, with results that were significantly better in comparison with the cisplatin group (Table 2).

NGF circulating levels were significantly reduced after cisplatin treatment in comparison with controls (mean 42.7 ng/ml ± SD 7.1 *versus* 69.4 ± 12.7, respectively; $P < 0.05$). In the cisplatin + ALC group the reduction was less severe (58.1 ng/ml ± 15.3), and the value was not significantly different from that measured in the CTRL group.

Antitumor Activity Studies. The possibility of a direct interaction between ALC and paclitaxel or cisplatin was examined using several human cancer cell lines in *in vitro* cytotoxic tests. In all of these experiments ALC by itself had no antitumor activity. As shown in Table 3 a high dose of ALC (200 μg/ml corresponding to 1 mM) had no effect on paclitaxel or cisplatin cytotoxicity. In addition, various *in vivo* tumor models were investigated to evaluate the antitumor response to cisplatin and paclitaxel in combination with ALC. Results concerning the antitumor activity of cisplatin alone or in combination with ALC on the murine 3LL-tumor are reported in Table 4. The administration of cisplatin at 8 mg/kg i.v. produced a TVI of 60% in treated mice, with no toxic deaths and an ILS of 86%. The lowest dose of 6 mg/kg i.v. was less effective, producing a TVI of 46% and an ILS of 21%. Both of the doses significantly reduced the number of lung metastases, and the combination of ALC with cisplatin did not influence the antimetastatic or the antitumor effects of cisplatin.

Table 5 Antitumor activity of paclitaxel and cisplatin in combination with ALC on different human tumor cell xenografts in nude mice

Tumor line	ALC[a] (mg/kg)	Cisplatin[b] (mg/kg)	Paclitaxel[c] (mg/kg)	TVI%[d]	Lethal toxicity[e]
NCI-H460	100			18	0/8
Lung carcinoma		6		55	0/8
	100	6		62	0/8
		8		86	2/8
	100	8		83	0/8
IGROV-1	100			21	0/4
Ovarian carcinoma		6		57	0/4
	100	6		76[f]	0/5
			54	98	0/4
	100		54	98[f]	0/5
A2780	100			38	0/4
Ovarian carcinoma		6		95	0/5
	100	6		96[f]	0/4
	100			9	0/5
			54	98	0/5
	100		54	97[f]	0/5
LoVo	100			0	0/5
Colon carcinoma			54	88	1/5
	100		54	90	0/5

[a] p.o., daily × 18, starting 3 days before the cytotoxic drug.
[b] i.v., every 7th day × 3 times.
[c] i.v., every 3rd–4th day × 4 times.
[d] Tumor volume inhibition % in treated *versus* control mice measured 7 days after the end of treatments.
[e] Number of mice dead from toxicity/total number of mice.
[f] ns, not significant

Table 5 shows the results of the studies designed to investigate the influence of ALC on the antitumor activity of cisplatin or paclitaxel in human tumor xenografts. Against the NCI-H460 human tumor xenograft the two doses of cisplatin, 6 and 8 mg/kg, were effective in inhibiting tumor growth (TVI% 55 and 86, respectively), and the combination with ALC did not influence the antitumor effects. In contrast, ALC showed a protective

Table 4 Effect of cisplatin i.v. (q2dx2) in combination with ALC p.o. (qdx14) on tumor growth, on median survival time, and on development of metastases in C57/BL6J male mice bearing a transplantable 3LL lung carcinoma

Cisplatin was administered one day after the tumor injection. ALC treatment started on the same day as tumor injection.

Treatment	Dose (mg/kg)	BWL%[a] max	TVI%[b]	MST[c] (range in days)	ILS%	Metastases/ lungs ± SE
Controls[d]	—	0	—	14 (14–24)	—	8.0 ± 1.1
ALC	100	0	2	17 (13–23)	21	6.7 ± 0.3
Cisplatin	6	5	46	17 (14–27)	21	[e]1.3 ± 0.8
ALC + cisplatin	100 + 6	11	40	[f]20 (14–23)	43	[e]2.5 ± 0.9
Cisplatin	8	11	60	[g]26 (18–29)	86	[e]1.1 ± 0.7
ALC + cisplatin	100 + 8	10	63	[g]26 (15–28)	86	[e]0.7 ± 0.5

[a] BWL%, maximum body weight loss during the experimental period.
[b] TVI, tumor volume inhibition was calculated 8 days after the last treatment with cisplatin.
[c] MST, median survival time (days).
[d] Controls, vehicle-treated group.
[e] $P < 0.01$ *versus* vehicle (Mann-Whitney).
[f] $P < 0.05$ *versus* vehicle (Mann-Whitney).
[g] $P < 0.001$ *versus* vehicle (Mann-Whitney).

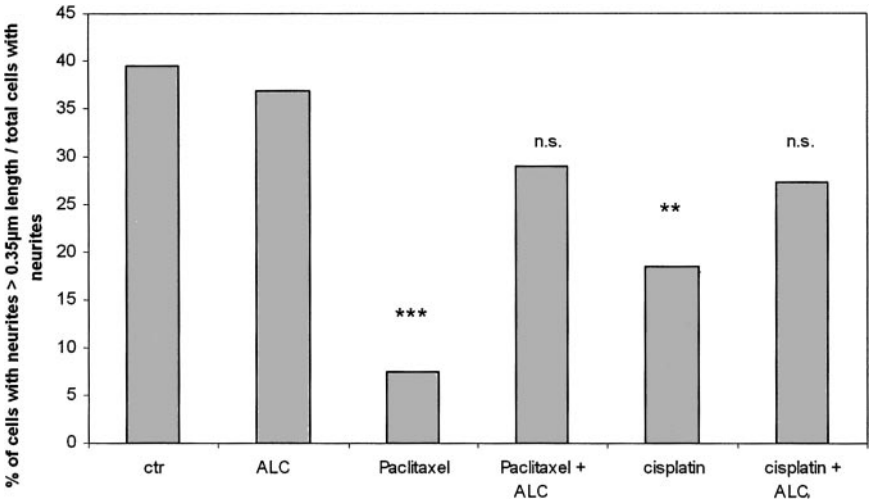

Fig. 1 PC12 cells were seeded in six-well plates at a density of 150,000 cells/well. After 6 h cells were treated with NGF 100 ng/ml for 72 h. At the end of the period of incubation the medium was replaced, and the differentiated cells were treated with NGF 100 ng/ml ± 1 μg/ml paclitaxel, 10 μg/ml cisplatin, and ± 1 mM ALC for 24 h, and processed as described in "Materials and Methods." Statistical analysis (ANOVA test): *** $P < 0.001$ *versus* controls (*ctr*) and ALC; ** $P < 0.01$ *versus* ctr and ALC; n.s., not significant *versus* ctr and ALC.

effect on the lethal toxicity induced by the highest dose of cisplatin (8 mg/kg), which was well tolerated in the combination, whereas it caused 2 of 5 dead mice when administered by itself. Again, ALC failed to modify the antitumor effects of cisplatin against the IGROV-1 and the A2780 human ovarian carcinomas. The best regimen of paclitaxel (54 mg/kg, i.v. every 4th day for four times) was also tested in these tumors, resulting in a very high tumor inhibition (TVI% 98) either alone or in combination with ALC (Table 5). No influence of ALC on paclitaxel antitumor effects was observed in the A2780 human ovarian and in the LoVo colon carcinoma xenografts.

ALC Reduces Neurite Damage in Paclitaxel and Cisplatin PC12-Treated Cells. To investigate the neuroprotective effect of ALC at the cellular level we performed *in vitro* experiments using rat pheochromocytoma PC12 cells. Cells were treated with 100 ng/ml of NGF for 72 h to induce neuronal differentiation. Then, differentiated PC12 cells were incubated with cisplatin or paclitaxel ± 1 mM ALC for 24 h in the presence of fresh NGF (100 ng/ml). The percentage of neurites of differentiated cells (*i.e.,* neurites >0.35 μm) was drastically decreased in paclitaxel-treated cells with respect to the controls (7% *versus* 39%, respectively; $P < 0.001$; Fig. 1). The reduction in the percentage of differentiated cells was evident also in the cisplatin-treated cells *versus* controls, although to a lesser extent (19% *versus* 39%, respectively; $P < 0.01$). Conversely, the ALC cotreatment with paclitaxel or cisplatin reduced the toxic effect on neurite elongation (differences were not significant with respect to the control group; Fig. 1). No differences between the controls and ALC-treated cells were observed.

Synergy between NGF and ALC in Promoting Gene Expression. Previous reports indicate that ALC can act synergistically with low suboptimal amounts of NGF (1 ng/ml) in triggering differentiation of neuronal cells (38). To additionally investigate, at the molecular level, the putative role of ALC in increasing NGF-responsive gene activation, we analyzed the PC12 transcription pattern using a Clonthec microarray filter system. In these experiments, the pattern of gene expression of PC12 cells treated with 1 ng/ml NGF, or 1 mM ALC or 1 mM ALC plus 1 ng/ml NGF was compared (Table 6). Interestingly, the expression of several genes was up-regulated in NGF plus ALC cotreated cells. A marked up-regulation was observed for VG F8A and NGFI-A (also known as zif 268, Egr 1, Krox 24, PC1, TIS g, and d2), two genes characterized by their responsiveness to NGF (39–42). This modulation was confirmed by Northern blot analysis of NGFI-A expression (Fig. 2). In this experiment we analyzed over the course of time (1, 2, and 4 h) the expression of NGFI-A and c-myc (another well-known NGF early responsive gene) after treatments with ALC, or 1 ng/ml NGF ± ALC and/or 100 ng/ml NGF.

The results showed that the addition of 1 mM ALC alone has no effect, whereas 1 ng/ml NGF produces only a slight increase in NGFI-A transcription (Fig. 2). However, when the cells were simultaneously treated for 1 h with both 1 mM ALC and 1 ng/ml NGF, the expression of NGFI-A mRNA was increased >10-fold with respect to untreated cells, although it was still lower than in cells treated with 100 ng/ml NGF (Fig. 2). This result supports, at the molecular level, the ability of ALC to enhance NGFI-A transcription induced by NGF. Conversely, the transcription of the c-myc gene seemed not to be influenced by the presence of ALC (Fig. 2).

The Acetyl Group Associated with ALC Is Transferred to Histones. To clarify whether up-regulation of gene expression occurring on treatment with ALC could be correlated with increased acetylation level of histones as suggested by Fanti *et al.* (21), the levels of endogenous acetylated histone H4 in differentiating PC12 cells was quantified after 1 h of treatment with 1 mM ALC (Fig. 3). Neither 1 ng/ml NGF nor 1 mM ALC alone produced any variation in the level of acetylated histone H4, whereas the amount achieved in cell cultures simultaneously treated with 1 mM ALC and 1 ng/ml NGF was comparable with that of cells treated with 100 ng/ml NGF alone (20% increase with respect to untreated cells; $P < 0.01$). Therefore, these data provide direct evidence that the addition of ALC plus a low dose of NGF (1 ng/ml) acts as an enhancer of histone H4 hyperacetylation.

Finally, to understand whether the ALC-deriving acetyl groups can be directly retained on chromatin, we pulse-labeled confluent PC12 cells with 10 μCi/ml [^{14}C]ALC la-

Table 6 PC12 transcription pattern using a microarrays filter system

In these experiments, the pattern of gene expression of untreated cells (ctr) was compared with 1 ng/ml NGF, 1 mM ALCAR, or 1 mM ALCAR plus 1 ng/ml NGF of 2-h treated PC12 cells.

GenBank accession no.	Protein/gene	Modulation of gene expression by treatments[a]		
		1 mM ALCAR	1 ng/ml NGF	1 ng/ml NGF + 1 mM ALCAR
M20035;	prothymosin-alpha (PTMA)	+	/	+
D10754	proteasome delta subunit precursor; macropain delta; multicatalytic endopeptidase complex delta; proteasome subunit Y; proteasome subunit 5; PSMB6	+	/	+
M86389	heat shock 27-kDa protein (HSP27)	−	/	/
J03752	microsomal glutathione S-transferase (GST12; MGST1)	+	/	+
U43175	ATPase, subunit F, vacuolar (vatf)	+	/	/
K02933	40S ribosomal protein S17 (RPS17)	+	+	/
D44495	apurinic/apyrimidinic endonuclease (AP endonuclease; APEX; APEN)	+	/	/
D10864	Id-3; DNA-binding protein inhibitor; HLH protein	/	+	+
X06942	A-raf proto-oncogene	/	+	/
D12771	fibroblast ADP/ATP carrier protein; ADP/ATP translocase 2; adenine nucleotide translocator 2 (ANT2)	/	+	/
M60525	VGF8A protein precursor	/	+	++
D38222	Tyrosine phosphatase-like protein; negative regulator of PTPases in neuronal tissues, RAT PHEOCHROMOCYTOMA-DERIVED PROTEIN TYROSINE PHOSPHATASE-LIKE PROTEIN (EC 3.1.3.48)	/	+	+
D10862	DNA-binding protein inhibitor ID1	/	/	+
D10863	Id-2; DNA-binding protein inhibitor; HLH protein	/	/	+
X16956 + U26663	microglobulin; beta-2-microglobulin + prostaglandin receptor F2a	/	/	+
D13123	ATP synthase lipid-binding protein P1 precursor; ATPase protein 9; ATP5G1	/	/	+
X64827	cytochrome c oxidase, subunit VIIIh	/	/	+
D10021	mitochondrial ATP synthase D subunit; ATP5H	/	/	+
M19044	mitochondrial ATP synthase beta subunit precursor (ATP5B)	/	/	+
X51707	S19; 40S ribosomal protein S19	/	/	+
M84716	Fte-1; putative v-fos transformation effector protein; yeast mitochondrial protein import homolog; 40S ribosomal protein S3A; RPS3A	/	/	+
X06832	chromogranin A	/	/	+
M18416; J04154	early growth response protein 1 (EGR1); nerve growth factor-induced protein A (NGFI-A)	/	/	++
L07578	Casein kinase I delta; CKId; 49-kDa isoform	/	/	+
D17615	14-3-3 protein zeta/delta; PKC inhibitor protein-1; KCIP-1; mitochondrial import stimulation factor S1 subunit	/	/	+
L12384	ADP-ribosylation factor 5 (ARF5)	/	/	+

[a] Symbols indicate how many fold the particular gene was modulated by treatment: / = not modulated; + = up-regulated >2-fold; ++ = up-regulated >5-fold.

beled on the acetyl group for 30 min, and we simultaneously induced them to differentiate by treatment with 100 ng/ml of NGF. The results clearly show that histones H3 and H4 were strongly labeled both in ALC and acetate-treated cells (Fig. 4), thereby indicating that ALC can act as a donor molecule of acetyl groups to histones.

DISCUSSION

The prevention of chemotherapy-induced neuropathy associated with the clinical use of cisplatin and paclitaxel is thus far an unsolved issue. In this study we reported that ALC, a natural compound already known for having a protective effect against the myocardial toxicity produced by antineoplastic agents (43), was able to reduce the severity of cisplatin and paclitaxel neurotoxicity in well-established animal models (24–26, 38). Moreover, ALC did not interfere with the antineoplastic activity of both drugs, as assessed in several *in vitro* and *in vivo* tumor systems.

The explanation for the different sensitivity to ALC protection in tumor cells and in normal tissues is still only speculative. Because ALC is implicated in different aspects of intermediary metabolism (11–14), it is possible that some of the mechanisms and biochemical pathways modulated by this agent may have tissue-specific relevance. Of all of the various possibilities, we focused our attention primarily on the interaction between NGF, extensively studied as a neuroprotective agent in relation to cisplatin and paclitaxel neurotoxicity (6–8, 10, 44–48), and ALC. Our results indicate that ALC is able to potentiate the effect of NGF on PC12 cells by enhancing the expression of different genes, as assessed by microarray analysis, and a relationship between NGF and ALC in promoting PC12 neuritis outgrowth was also reported (39). Another definite relationship between ALC and NGF was found in the animal model of chronic cisplatin-induced sensory neuropathy. In this model, a close relationship has already been demonstrated between the onset of a sensory neuropathy and the decrease in NGF circulating levels (4). Here, ALC cotreatment significantly reduced the severity of cisplatin-induced sensory neuropathy, and ac-

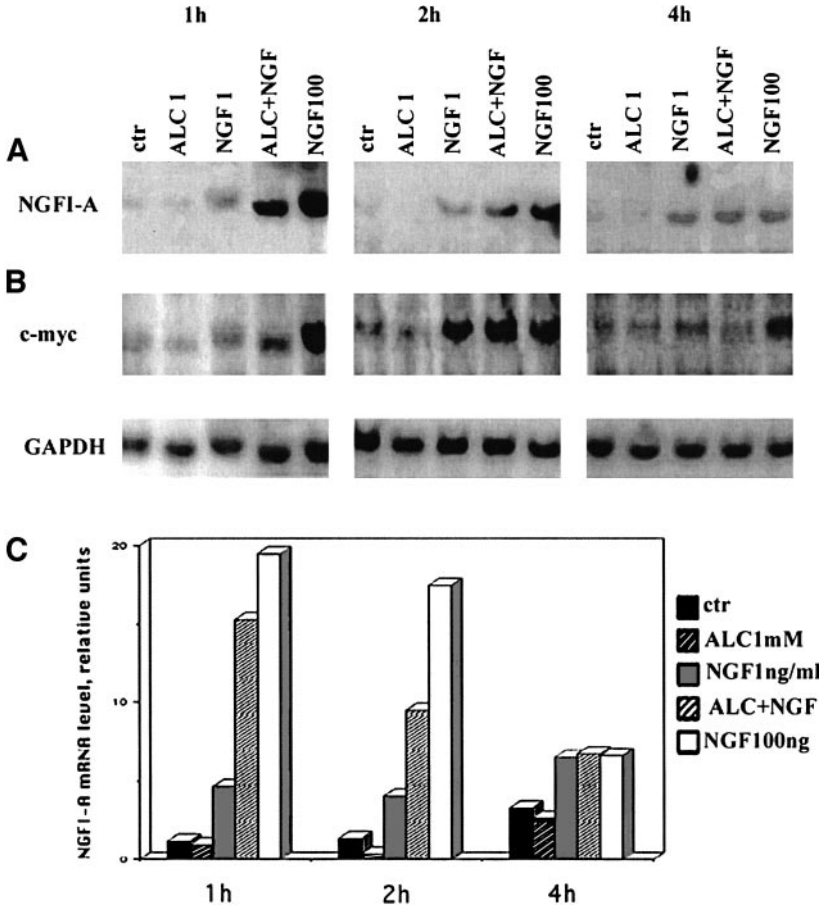

Fig. 2 Northern analysis of NGFI-A (*A*) and c-myc (*B*) during PC12 cell differentiation. Cells were untreated (*ctr*) or treated for 1, 2, and 4 h with 1 mM ALC, 1 ng/ml NGF, 1 mM ALC plus 1 ng/ml NGF, and 100 ng/ml NGF. Densitometric analysis (*C*) reveals that 1 h of treatment with 1 ng/ml NGF plus 1 mM ALC induces a 10-fold increase in the expression of NGFI-A mRNA compared with controls. Instead, in ALC-treated cells, no significant variation in the expression of proliferation-responsive c-myc gene was observed.

cordingly, the circulating levels of NGF were significantly higher in the ALC cotreated rats than in cisplatin-treated rats. These data are in agreement with the results reported previously, which, in various animal models, demonstrated that the exogenous administration of NGF was able to reduce the severity of cisplatin-induced peripheral neurotoxicity (3, 6–8).

A significantly reduced severity of neuropathy was also observed in the *in vivo* model of paclitaxel neurotoxicity in the paclitaxel-ALC treated group. In this animal model we did not search for any change in the circulating levels of NGF because, in our previous study on the time course of NGF circulating level changes during chronic cisplatin treatment, a significant difference in NGF level was observed only starting from 20 days after the beginning of drug administration (4), whereas our paclitaxel model is a short-term model (*i.e.*, 12 days). However, the importance of NGF in long-term paclitaxel neurotoxicity is clearly evidenced in the study by Apfel *et al.* (49), which shows a significant neuroprotective action of the exogenous administration of NGF in a chronic mouse model of paclitaxel neuropathy.

In addition to the effect of reducing the NGF fall in cisplatin-treated animals, ALC seems to increase the cell response to NGF as emerged from our *in vitro* experiments.

Regarding the molecular mechanisms that are the basis for the protective effect of ALC, this study showed the ability of the protective agent to enhance the neuronal NGF response via histone acetylation, a mechanism that is involved in the regulation of gene expression (50–53). According to this hypothesis, we have shown that the acetyl group of ALC is transferred to histones in NGF-differentiated PC12 cells. We have also demonstrated that the presence of ALC increased NGF-induced histone acetylation. Moreover, the addition of ALC to PC12 cells significantly stimulated the expression of NGFI-A, a gene coding for a transcription factor with tumor suppressor effects (54–56). In addition, NGFI-A protein is implicated in several physiological processes, and it has been suggested that it may play an important role in tissue repair (57). Conversely to the positive regulation of NGFI-A, ALC treatment did not increase the transcription of the c-myc gene. Because the c-myc transcription is insensitive to chromatin acetylation, as shown by O'Neill and Turner (58), our observation additionally supports the suggestion that ALC does not affect the genes of which the expression is not linked to histone modification. The levels of acetylation of histones are regulated by two classes of counteracting enzymes: the histone-acetyltransferases, which promote the transfer of acetyl groups to histones (59–62), and the histone-specific deacetylases, which remove acetyl groups from histones (60, 63, 64). It is generally accepted that histone-acetyltransferases use acetyl-CoA as their substrate (59, 65). Although being of great relevance, the molecular mechanisms

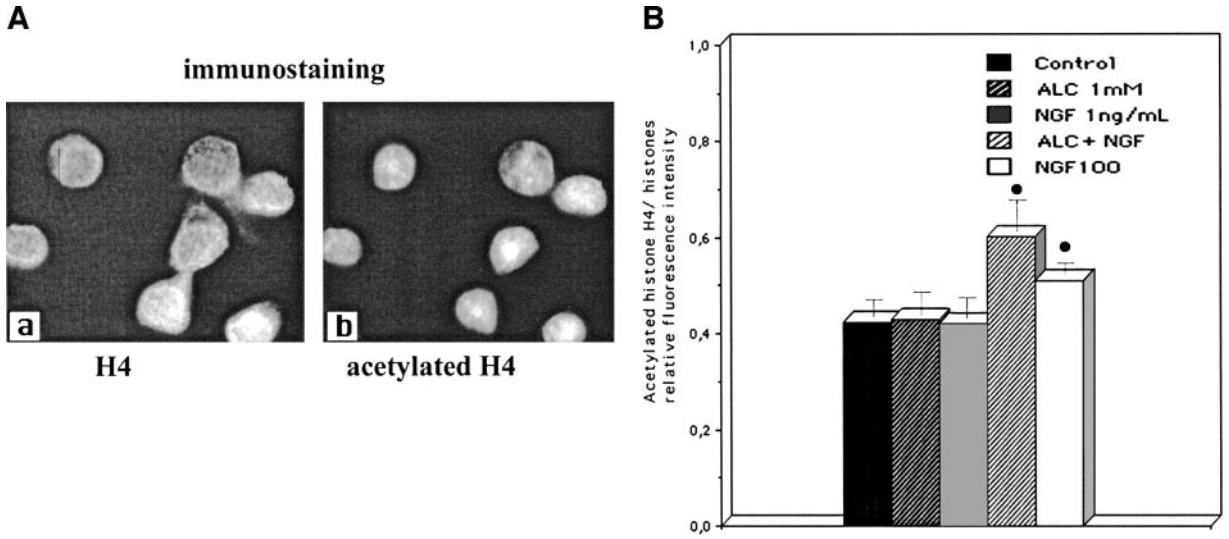

Fig. 3 *A*, example of double immunostaining using polyclonal antihistone H4 antibody direct against an antigen determinant present on H4 histone protein (*a*) and a polyclonal antiacetylated histone H4 antibody (*b*) in PC12 cells. *B*, densitometric analysis of the fluorescence associated with the antiacetylated histone H4 antibody normalized to the corresponding fluorescence obtained with the antihistone antibody. Cells were untreated (*control*) or treated for 1 h with 1 mM ALC, 1 ng/ml NGF, 1 mM ALC plus 1 ng/ml NGF, and 100 ng/ml NGF, and then processed for double immunostaining. As shown, the intensity of the fluorescence associated with the antiacetylated histone H4 antibody is increased in cells exposed to both 100 ng/ml NGF and 1 mM ALC plus 1 ng/ml NGF. Each mean value represents the fluorescence intensity of 100 nuclei; *bars*, ± SE. Three slides for each treatment group were scored in two independent experiments. Statistical analysis (ANOVA test): ● $P < 0.01$ *versus* control, NGF 1 ng/ml, and ALC 1 mM.

regulating the nuclear concentration of acetyl-CoA remain as yet largely unknown. Because a well-documented function of physiological ALC is the regulation of the cellular levels of acetyl-CoA (12, 14, 66), we hypothesize that the exogenous administration of ALC may indirectly modulate the process of acetylation of histones by regulating the nuclear levels of acetyl-CoA. In light of this, it is tempting to speculate that hyperacetylation of histones occurring on treatment with ALC in the presence of low levels of NGF (as occurs in chemotherapy-induced neuropathy; Ref. 2) may lead to up-regulation of genes of which the expression is required to counteract the toxicity of antineoplastic drugs.

In conclusion, our results indicate that ALC is a specific protective agent for chemotherapy-induced neuropathy after cisplatin or paclitaxel treatment. Relevant to this point is the lack of any interference with the antitumor activity of the drugs. Moreover, ALC, a substance already in clinical use with various indications, is safe and extremely well tolerated. Finally, there is considerable evidence suggesting that ALC can enhance the supportive effect of physiological NGF during chemotherapy-induced neuropathy, thus avoiding the problem of the local and general side effects of the exogenous administration of NGF, which are a major problem of this neuroprotective strategy (49).

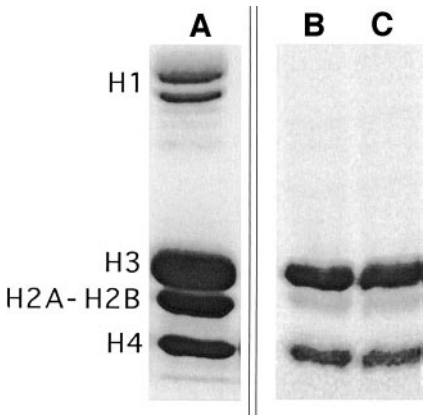

Fig. 4 *A*, SDS-PAGE and Coomassie staining of histones purified from PC12 nuclei. *B* and *C*, SDS-PAGE and autoradiography of the histone fraction purified from PC12 cells treated with [^{14}C]ALC (*B*) and [^{14}C]acetate (*C*). Both molecules label histones H3 and H4.

AKNOWLEDGMENTS

We thank Dr. Maria L. Cervoni, Dr. Fabiana F. Ferrara, Angelo Marconi, Patrizia Tobia, and Eleonora Barazzetta for excellent technical assistance, and Dr. Elizabeth Genton for manuscript revision.

REFERENCES

1. Meijer, C., de Vries, E. G., Marmiroli, P., Tredici, G., Frattola, L., and Cavaletti, G. Cisplatin-induced DNA platination in experimental dorsal root ganglia neuronopathy. Neurotoxicology, *20:* 883–887, 1999.

2. De Santis, S., Pace, A., Bove, L., Cognetti, F., Properzi, F., Fiore, M., Triaca, V., Savarese, A., Simone, M. D., Jandolo, B., *et al.* Patients treated with antitumor drugs displaying neurological deficits are characterized by a low circulating level of nerve growth factor. Clin. Cancer Res., *6:* 90–95, 2000.

3. Aloe, L., Manni, L., Properzi, F., De Santis, S., and Fiore, M. Evidence that nerve growth factor promotes the recovery of peripheral neuropathy induced in mice by Cisplatin: behavioral, structural and biochemical analysis. Auton. Neurosci., *86:* 84–93, 2000.

4. Cavaletti, G., Pezzoni, G., Pisano, C., Oggioni, N., Sala, F., Zoia, C., Ferrarese, C., Marmiroli, P., and Tredici, G. Cisplatin-induced peripheral neurotoxicity in rats reduces the circulating levels of nerve growth factor. Neurosci. Lett., *322:* 103–106, 2002.

5. Apfel, S. C. Neurotrophic factors in peripheral neuropathies: therapeutical implications. Brain Pathol., *9:* 393–413, 1999.

6. Apfel, S. C., Arezzo, J. C., Lipson, L. A., and Kessler, J. A. Nerve growth factor prevents experimental cisplatin neuropathy. Ann. Neurol., *31:* 76–80, 1992.

7. Schmidt, Y., Unger, I., Bartke, R., and Reiter, R. Effect of nerve growth factor on peptide neurons in dorsal root ganglia after taxol or cisplatin treatment and in diabetic (cd/db) mice. Exp. Neurol., *132:* 16–23, 1995.

8. Tredici, G., Braga, M., Nicolini, G., Miloso, M., Marmiroli, P., Schenone, A., Nobbio, L., Frattola, L., and Cavaletti, G. Effect of recombinant human nerve growth factor on cisplatin neurotoxicity in rats. Exp. Neurol., *159:* 551–558, 1999.

9. Moos, P. J., and Fitzpatrick, F. A. Taxane-mediated gene induction is independent of microtubule stabilization: induction of transcription regulators and enzymes that modulate inflammation and apoptosis. Proc. Natl. Acad. Sci. USA, *95:* 3896–3901, 1998.

10. Apfel, S. C., Lipton, R. B., Arezzo, J. C., and Kessler, J. A. Nerve growth factor prevents toxic neuropathy in mice. Ann. Neurol., *29:* 87–90, 1991.

11. Fritz, I. B. Carnitine and its role in fatty acid metabolism. Adv. Lipid Res., *1:* 285–334, 1963.

12. Bremer, J. Carnitine metabolism and functions. Physiol. Rev., *63:* 1420–1480, 1983.

13. Stanley, C. A. New genetic defects in mitochondrial fatty acid oxidation and carnitine deficiency. Adv. Pediatr., *34:* 59–88, 1987.

14. Bieber, L. L. Carnitine. Annu. Rev. Biochem., *57:* 261–283, 1988.

15. Lowitt, S., Malone, J. I., Salem, A. F., and Korthals, J., Benford, S. Acetyl-L-carnitine corrects the altered peripheral nerve function of experimental diabetes. Metabolism, *44:* 677–680, 1995.

16. Di Giulio, A. M., Lesma, E., and Gorio, A. Diabetic neuropathy in the rat: 1. ALC augments the reduced levels and axoplasmic transport of substance P. J. Neurosci. Res., *40:* 414–419, 1995.

17. Kano, M., Kawakami, T., Hori, H., Hashimoto, Y., Tao, Y., Ishikawa, Y., and Takenaka, T. Effects of ALC on the fast axoplasmic transport in cultured sensory neurons of streptozotocin-induced diabetic rats. Neurosci. Res., *33:* 207–213, 1999.

18. Fernandez, E., Pallini, R., Tamburrini, G., Lauretti, L., Tancredi, A., and La Marca, F. Effects of levo-acetylcarnitine on second motoneuron survival after axotomy. Neurol. Res., *17:* 373–376, 1995.

19. Piovesan, P., Pacifici, L., Taglialatela, G., Ramacci, M. T., and Angelucci, L. Acetyl-L-carnitine treatment increases choline acetyltransferase activity and NGF levels in the CNS of adult rats following total fimbria-fornix transection. Brain Res., *633:* 77–82, 1994.

20. Foreman, P. J., Perez-Polo, J. R., Angelucci, L., Ramacci, M. T., and Taglialatela, G. Effect of Acetyl-L-carnitine treatment and stress exposure on the nerve growth factor receptor ($p75^{NGFR}$) mRNA level in the central nervous system of aged rats. Prog. Neuropsychopharmacol. Biol. Psych., *19:* 117–133, 1995.

21. Fanti, L., Berloco, M., and Pimpinelli, S. Carnitine suppression of position-effect variegation in Drosophila melanogaster. Mol. Gen. Genet., *244:* 588–595, 1994.

22. Pomponi, M. G., and Neri, G. Butyrate and Acetyl-l-carnitine inhibit the Cytogenetic expression of the fragile X *in vitro.* Am. J. Med. Gen., *51:* 447–450, 1994.

23. Cavaletti, G., Cavalletti, E., Montaguti, P., Oggioni, N., De Negri, O., and Tredici, G. Effect on the peripheral nervous system of the short-term intravenous administration of paclitaxel in the rat. Neurotoxicology, *18:* 137–146, 1997.

24. Cavaletti, G., Tredici, G., Marmiroli, P., Petruccioli, M. G., Barajon, I., and Fabbrica, D. Morphometric study of the sensory neurones and peripheral nerve changes induced by chronic cisplatin (DDP) administration. Acta Neuropathol., *84:* 364–371, 1992.

25. Cavaletti, G., Minoia, C., Schieppati, M., and Tredici, G. Protective effects of glutathione on cisplatin neurotoxicity in rats. Int. J. Radiat. Oncol. Biol. Phys., *29:* 771–776, 1994.

26. Tredici, G., Cavaletti, G., Petruccioli, M. G., Fabbrica, D., Tedeschi, M., and Venturino, P. Low-dose glutathione administration in the prevention of cisplatin-induced peripheral neuropathy in rats. Neurotoxicology, *15:* 701–704, 1994.

27. Skehan, P., Stoneng, R., Scudiero, D., Monks, A., Mc Mahon, J., Vistica, D., Warren, J. T., Bokesch, H., Kennedy, S., and Boyd, M. R. New colorimetric cytotoxicity assay for anticancer-drug screening. J. Natl. Cancer Inst., *82:* 1107–1112, 1990.

28. Pratesi, G., Manzotti, C., Tortoreto, M., Prosperi, E., and Zunino, F. Effects of 5-FU and *cis*-DDP combination on human colorectal tumor xenografts. Tumori, *75:* 60–65, 1989.

29. Geldof, A. A. Nerve-growth-factor-dependent neurite outgrowth assay; a research model for chemotherapy-induced neuropathy. J. Cancer Res. Clin. Oncol., *121:* 657–660, 1995.

30. Land, H., Parada, L. F., and Weinberg, R. A. Tumorigenic conversion of primary embryo fibroblasts requires at least two cooperating oncogenes. Nature (Lond.), *304:* 596–602, 1983.

31. Caruso, M., Martelli, F., Giordano, A., and Felsani, A. Regulation of MyoD gene transcription and protein function by the transforming domains of the adenovirus E1A oncoprotein. Oncogene, *8:* 267–278, 1993.

32. Tirone, F., and Shooter, E. M. Early gene regulation by nerve growth factor in PC12 cells: induction of an interferon-related gene. Proc. Natl. Acad. Sci. USA, *86:* 2088–2092, 1989.

33. Lin, R., Leone, J. W., Cook, R. G., and Allis, C. D. Antibodies specific to acetylated histones document the existence of deposition- and transcription-related histone acetylation in Tetrahymena. J. Cell Biol., *108:* 1577–1588, 1989.

34. Arends, M. J., Morris, R. G., and Wyllie, A. M. Apoptosis, the role of the endonucleases. Am. J. Pathol., *3:* 593–608, 1990.

35. van der Westhuyzen, D. R., Bohm, E. L., and von Holt, C., Fractionation of chicken erythrocyte whole histone into the six main components by gel exclusion chromatography. Biochim. Biophys. Acta, *359:* 341–345, 1974.

36. Laemmli, U. Cleavage of structural proteins during the assembly of the head of bacteriophage T4. Nature (Lond.), *227:* 680–685, 1970.

37. Bradford, M. A rapid and sensitive method for the quantitation of microgram quantities of protein utilizing the principle of protein-dye binding. Anal. Biochem., *72:* 248–254, 1976.

38. Taglialatela, G., Angelucci, L., Ramacci, M. T., Werrbach-Perez, K., Jackson, G. R., and Perez-Polo, R. Stimulation of nerve growth factor receptor in PC12 cells by acetyl-l-carnitine. Biochem. Pharmacol., *44:* 577–585, 1992.

39. Sussman, M. A., Battenberg, E., Bloom F. E., and Fowler, V. M. Identification of two nerve growth factor-induced polypeptides in PC12 cells. J. Mol. Neurosci., *2:* 163–174, 1990.

40. Milbrandt, J. A nerve growth factor-induced gene encodes a possible transcriptional regulatory factor. Science (Wash. DC), *238:* 797–800, 1987.

41. Lemaire, P., Revelant, O., Bravo, R., and Charney, P. Two mouse genes encoding potential transcription factors with identical DNA-binding domains an activated by growth factors in cultured cells. Proc. Natl. Acad. Sci. USA, *85:* 4691–4695, 1988.

42. Janssen-Timmen, U., Lemaire, P., Mattei, M. G., Revelant, O., and Charnay, P. Structure, chromosome mapping and regulation of mouse zinc-finger gene Krox-24; evidence for a common regulatory pathway for immediate-early serum-response genes. Gene, *80:* 325–336, 1989.

43. Alberts, A. D., Peng, Y. M., Moon, T. E., and Bressler, R. Carnitine prevention of adriamycin toxicity in mice. Biomedicine, *29:* 265–268, 1978.

44. Eriksson, N. P., Lindsay, R. M., and Alskogius, H. BDNF and NT-3 rescue sensory but not motoneurons following axotomy in the neonate. Neuroreport, *5:* 1445–1448, 1994.

45. Gao, W. Q., Dybdal, N., Shinsky, N., Murnane, A., Schmelzer, C., Siegel, M., Keller, G., Hefti, F., Phillips, H. S., and Winslow, J. W. Neurotrophin-3 reverses experimental cisplatin-induced peripheral sensory neuropathy. Ann. Neurol., *38:* 30–37, 1995.

46. Hayakawa, K., Soube, G., Itoh, T., and Mitsuma, T. Nerve growth factor prevents neurotoxic effects of cisplatin, vincristine and taxol on adult rat sympathetic ganglion explants *in vitro*. Life Sci., *54:* 519–525, 1994.

47. Malgrange, B., Delrée, P., Rigo, J. M., Baron, H., and Moonen, G. Image analysis of neurite regeneration by adult rat dorsal root ganglion neurons in culture: quantification of the neurotoxicity of anticancer agents and its prevention by nerve growth factor or fibroblast growth factor but not brain-derived neurotrophic factor or neurotrophin-3. J. Neurosci. Meth., *53:* 111–122, 1994.

48. Windebank, A. J., Smith, A. G., and Russell, J. W. The effect of nerve growth factor, ciliary neurotrophic factor, and ACTH analogs on cisplatin neurotoxicity *in vitro*. Neurology, *44:* 488–494, 1994.

49. Apfel, S. C., Kessler, J. A., Adornato, B. T., Litchy, W. J., Sanders, C., Rask, C. A. and the NGF Study Group. Recombinant human nerve growth factor in the treatment of diabetic polyneuropathy. Neurology, *51:* 695–702, 1998.

50. Grunstein, M. Histone function in transcription. Annu. Rev. Cell Biol., *6:* 643–678, 1990.

51. Morse, R. H. Transcribed chromatin. Trends Biochem. Sci., *17:* 23–26, 1992.

52. Turner, B. M. Decoding the nucleosome. Cell, *75:* 5–8, 1993.

53. Turner, B. M., and O'Neill, L. P. Histone acetylation in chromatin and chromosomes. Semin. Cell Biol., *6:* 229–236, 1995.

54. Huang, R. P., Liu, C., Fan, Y., Mercola, D., and Adamson, E. D. Egr-1 negatively regulates human tumor cell growth via the DNA-binding domain. Cancer Res., *55:* 5054–5062, 1995.

55. Huang, R. P., Fan, Y., de Belle, I., Niemeyer, C., Gottardis, M. M., Mercola, D., and Adamson, E. D. Decreased Egr-1 expression in human, mouse and rat mammary cells and tissues correlates with tumor formation. Int. J. Cancer, *72:* 102–109, 1997.

56. Huang, R. P., Darland, T., Okamura, D., Mercola, D., and Adamson, E. D. Suppression of v-sis-dependent transformation by the transcription factor, Egr-1. Oncogene, *9:* 1366–1377, 1994.

57. Braddock, M. The transcription factor Egr-1: a potential drug in wound healing and tissue repair. Brain Res. Rev., *28:* 370–490, 1998.

58. O'Neill, L. P., and Turner, B. M. Histone H4 acetylation distinguishes coding regions of the human genome from heterochromatin in a differentiation-dependent but transcription-independent manner. EMBO J., *14:* 3946–3957, 1995.

59. Mamorstein, R., and Roth, S. Y. Histone acetyltransferases: function, structure and catalysis. Curr. Opin. Genes Dev., *11:* 155–161, 2001.

60. Strahl, B. D., and Allis, C. D. The language of covalent histone modifications. Nature (Lond.), *403:* 41–45, 2000.

61. Grunstein, M., Histone acetylation in chromatin structure and transcription. Nature (Lond.), *389:* 349–352, 1997.

62. Sterner, D. E., and Berger, S. L. Acetylation of histones and transcription-related factors. Microbiol. Mol. Biol. Rev., *64:* 435–459, 2000.

63. Kuo, M. H., and Allis, C. D. Roles of histone acetyltransferases and deacetylases in gene regulation. Bioessays, *20:* 615–626, 1998.

64. Pazin, M. J., and Kadonaga, J. T. What's up and down with histone deacetylation and transcription? Cell, *89:* 325–328, 1997.

65. Loidl, P. Histone acetylation: facts and questions. Chromosoma, *103:* 441–449, 1994.

66. Rebouche, C. J., and Paulson, D. J. Carnitine metabolism and function in humans. Annu. Rev. Nutr., *6:* 41–66, 1986.

Clinical Cancer Research

Paclitaxel and Cisplatin-Induced Neurotoxicity: A Protective Role of Acetyl-L-Carnitine

Claudio Pisano, Graziella Pratesi, Diletta Laccabue, et al.

Clin Cancer Res 2003;9:5756-5767.